

Synergistic Passive Cooling of Photovoltaics: A Numerical Study on Combining Radiative Cooling and Hydrogel-based Evaporative Cooling

Weijian Lin¹, Tao Li¹, Tao Ma^{1*}

1 Engineering Research Centre of Solar Energy and Refrigeration of MOE, School of Mechanical Engineering, Shanghai Jiao Tong University, Shanghai, China

*(Corresponding Author: tao.ma@sjtu.edu.cn)

ABSTRACT

Evaporative cooling using hygroscopic composite hydrogels and radiative cooling are widely studied passive thermal management strategies for photovoltaic (PV) modules. This work explores a synergistic approach that integrates evaporative cooling through a hygroscopic hydrogel on the back side with radiative cooling on the front side of PV modules. A highly accurate heat and mass transfer model is developed and validated to simulate three configurations: radiative cooling only; evaporative cooling only on the back side; and the combined use of both techniques. Results demonstrate that the hybrid configuration achieves the best cooling performance, yielding an average temperature reduction of 3.2 °C and power generation efficiency (PCE) increase by 1.2%, which corresponds to a 500% and 26% relative improvement in PCE compared to the radiative-cooling-only and evaporative-cooling-only cases, respectively. Notably, radiative cooling has only a minor influence on the hydrogel's absorption and desorption dynamics, increasing nighttime water absorption by about 1%, while the enhanced radiation extends the duration of the positive temperature reduction effect by 10%. Radiative cooling can be considered as a supplementary method coupled with PV modules, where evaporative cooling serves as the primary passive cooling mechanism.

Keywords: PV passive thermal management, evaporative cooling, radiative cooling, synergistic strategy

Nonmenclature

Abbreviations

EVA	Ethylene-Vinyl Acetate
PTFE	Polytetrafluoroethylene
PV	Photovoltaic

Symbols

A	contact area (m ²)
---	--------------------------------

a_w	water activity in salt solution
C	concentration (mol/m ³)
D	diffusion coefficient (m ² /s)
δ	thickness (m)
h	convective heat transfer coefficient (W/m ² /K)
j	water vapor flux (mol/m ² /s)
k	permeability of hydrogel (m ²)
k'	conductivity (W/m/K)
P	power (W/m ²)
ϕ	volume ratio (-)
R	universal gas constant
σ	Stefan Boltzmann constant
T	temperature (K)
u	wind speed (m/s)
ν	poisson's ratio of hydrogel (-)
G	hydrogel shear modulus (Pa)

1. INTRODUCTION

The rapid deployment of photovoltaic (PV) technology has positioned it as a cornerstone of the global transition to renewable energy [1]. However, the PCE of silicon-based PV modules is highly sensitive to temperature, with a typical power conversion efficiency decrease of 0.3–0.5% per degree Celsius rise above the standard test condition of 25°C [2]. In practice, PV modules often operate at temperatures exceeding 50°C, and even above 75°C in hot climates, leading to significant energy losses [3]. Therefore, developing effective and economical thermal management strategies for PV modules is of great significance.

PV thermal management methods can be classified into active and passive cooling, where passive cooling attracts attention with energy-free and low complexity [4]. Radiative cooling has emerged as one of passive cooling techniques, leveraging the transmission of thermal radiation through the atmospheric window (8–13 μ m) to outer space [5]. However, studies have shown

that the actual cooling effect is limited—typically less than 1°C under realistic outdoor conditions—due to the already high inherent emissivity of the glass encapsulation and the dominant role of convective heat transfer [6]. Even with ideal emissivity, the maximum temperature reduction is only about 1.8°C, making standalone radiative cooling economically unattractive for most commercial PV applications [7].

In contrast, evaporative cooling using hygroscopic hydrogels has demonstrated greater potential for immediate and substantial temperature reduction [8–10]. By absorbing atmospheric moisture and releasing it through evaporation, hydrogels leverage the high latent heat of water to provide maximum temperature reduction over 10°C [8]. These temperature drops significantly exceeding those achieved by radiative methods, particularly during peak solar hours and in well-ventilated conditions [6,11].

However, hydrogel-based evaporative cooling constrained by ambient humidity levels and the finite water reservoir, potentially leading to performance degradation in arid climates or over extended dry periods [12,13]. These limitations motivate the exploration of a synergistic hybrid cooling strategy. Radiative cooling functions continuously, day and night, while evaporative cooling provides intense, latent heat-driven cooling that is particularly effective during daytime heating. The combination of radiation and evaporation could lead to a more stable and lower operating temperature throughout the diurnal cycle than either method could achieve alone. It should be noted the combined strategy mentioned here is different from existing studies [14,15], where hydrogel is set on the front side of PV module and achieves radiation cooling and evaporative cooling simultaneously. The strategy discussed in this paper refers to combined radiation cooling and evaporative cooling realized by the front glass of PV module and by the hydrogel on the back respectively.

Motivated by this potential, we conduct a systematic numerical investigation to the combined cooling strategies. This study employs a comprehensive heat and mass coupling model to simulate and compare four specific PV module configurations: a standard base module, a module with only front-side radiative cooling, a module with only back-side evaporative cooling, and a hybrid module integrating both techniques. The primary objectives are to rigorously evaluate the individual and combined temperature reduction performance and to elucidate the heat dissipation pathways. The findings aim

to provide critical insights and a robust theoretical foundation for the development of combined passive thermal management systems for photovoltaics.

2. METHOD

2.1 Theoretical model

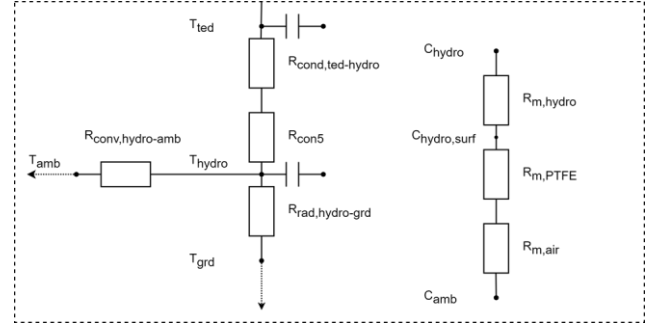


Fig. 1 Heat and mass transfer resistance diagram of model

A theoretical thermal resistance model is established based on the energy balance of the five components in a PV module: glass, EVA1, solar cell, EVA2, and tedlar [16]. For the specific case of evaporative cooling, the model is extended to incorporate the heat and mass transfer processes associated with a hygroscopic hydrogel layer, as illustrated in Fig. 1. Heat transfer resistance between tedlar and hydrogel consists of resistance of conduction $R_{\text{cond,ted-hydro}}$, which is calculated by Eq. (1), where δ , k' and A are thickness, conductivity and contact area respectively, and contact resistance R_{con5} , which is considered as constant of 1×10^{-4} K/W.

$$R_{\text{cond},i-j} = \frac{\delta_i}{2k'_i A_i} + \frac{\delta_j}{2k'_j A_j} \quad (1)$$

The radiative resistance to the ground $R_{\text{rad,hydro-grd}}$ is calculated by Eq. (2), where ϵ_{hydro} is the emissivity of hydrogel with value of 0.9. Temperature of ground T_{grd} is equal to the ambient temperature T_{amb} .

$$R_{\text{rad,hydro-grd}} = \frac{1}{\epsilon_{\text{hydro}} \sigma A (T_{\text{hydro}}^2 + T_{\text{grd}}^2) (T_{\text{hydro}} + T_{\text{grd}})} \quad (2)$$

The convective resistance to the ambient air is calculated by Eq. (3), where u being the wind speed.

$$R_{\text{conv,hydro-amb}} = \frac{1}{h_{\text{conv,hydro-amb}} A} \quad (3)$$

$$h_{\text{conv,hydro-amb}} = 2.8 + 3.0u$$

For mass transfer, the vapor concentration difference is the driving force (Eq. (4)). The mass transfer resistance of the hydrogel itself is defined as Eq.

(5), where the diffusion coefficient D_i within the hydrogel is calculated by Eq. (6) [17].

$$\Delta C = C_H - C_{amb} = \frac{a_w P_{sat}(T_{pv})}{RT_{pv}} - \frac{RH \times P_{sat}(T_{amb})}{RT_{amb}} \quad (4)$$

$$R_{m,hydro} = \frac{\delta_{hydro}}{D_i} \quad (5)$$

$$D_i = \frac{2(1-\nu)G}{(1-2\nu)\eta} k \quad (6)$$

$$k = \frac{k_0 \phi_s}{(1-\phi_s)^{1.5}}$$

The vapor evaporates from the hydrogel surface to the ambient is considered as a series connection which follows Eq. (7) and the resistance of the PTFE $R_{m,PTFE}$ and the resistance of the air boundary layer $R_{m,air}$ are calculated by Eq. (8).

$$j = \frac{C_H - C_{amb}}{\frac{\delta_{PTFE}}{D_{eff}} + \frac{\delta}{D_v}} = D_{eff} \frac{C_H - C_1}{\delta_{PTFE}} = D_v \frac{C_1 - C_{amb}}{\delta} \quad (7)$$

$$R_{m,PTFE} = \frac{\delta_{PTFE}}{D_{eff}} \quad (8)$$

$$R_{m,air} = \frac{\delta}{D_v}$$

2.2 Model validation

The predictive capability for temperature was validated against experimental data from a field test [8]. A representative temperature profile for a single day is shown in Fig. 2. The validation results demonstrate high accuracy, with the Root Mean Square Error (RMSE) and Mean Relative Error (MRE) for the PV module temperature being 0.98°C and 1.8%, respectively, for the case with the cooler, and 0.81°C and 1.4% for the case without the cooler. These low error values confirm that the model is sufficiently accurate for subsequent simulations.

3. RESULTS AND DISCUSSION

3.1 Comparison of cooling performance

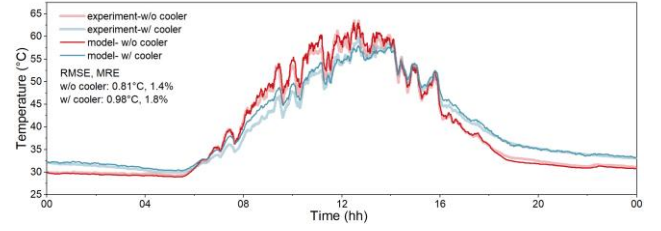


Fig. 2 Temperature profile of single day validation

Fig. 3 presents the temperature profiles and cooling performance of a PV module under four distinct configurations: a conventional PV module without cooling system (“w/o cooler”), a module equipped solely with radiative cooling (“w/ rad”), one with evaporative cooling only (“w/ evap”), and a module incorporating a hybrid cooling system combining both radiative and evaporative methods (“w/ hybrid”).

As illustrated in Fig. 3(a), the baseline module without cooling exhibits the highest operating temperatures, reaching approximately 62°C during peak hours. The integration of radiative cooling alone leads to a marginal average temperature reduction of 0.7°C (Fig. 3b), suggesting limited cooling capacity under the given environmental conditions. This observation aligns with findings reported in the literature [6], indicating that radiative cooling may not substantially lower temperatures when applied in isolation. In contrast, the evaporative cooling configuration demonstrated a more pronounced cooling effect, reducing the module temperature by an average of 2.5°C. This translated to a PV efficiency relative increase of 0.96%, which is 4.34 times greater than the 0.2% efficiency gain achieved by radiative cooling alone.

Notably, the hybrid cooling configuration achieves the most favorable thermal performance, with an average temperature reduction of 3.2°C. This result highlights a distinct synergistic effect between the radiative and evaporative cooling mechanisms. The

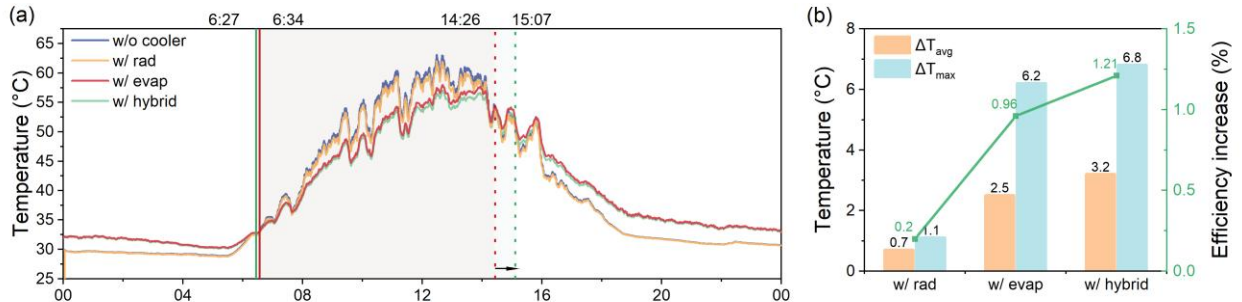


Fig. 3 (a): Temperature profile four configurations; (b): Cooling effects of three different configurations

combined approach not only enhances the instantaneous cooling effect but also prolongs the cooling duration—extending from 472 minutes with evaporative cooling alone to 520 minutes in the hybrid case. This extension is attributed to the complementary nature of the two methods: evaporative cooling provides immediate and potent heat removal, while radiative cooling contributes to sustained temperature regulation, particularly during periods of low evaporative efficiency. Quantitatively, this synergy translated into a remarkable 500% greater efficiency increase compared to radiative cooling alone, and a further 26% improvement over evaporative cooling by itself.

3.2 Comparison of energy distribution

Fig. 4 characterizes the cooling energy and synergistic effects achieved by integrating radiative and evaporative cooling. Fig. 4(a) illustrates the distribution of cooling energy at 12 p.m. across four system configurations. It is evident that the incorporation of hydrogel introduces a significant portion of cooling energy, comparable in magnitude to the radiative cooling contribution from the front surface. When the emissivity of the glass cover is increased to 1, a moderate enhancement in radiative cooling energy is observed in both the radiative cooling-only (w/ rad) and hybrid (w/ hybrid) configurations. Fig. 4(b) presents a temporal comparison of the contributions from radiative and evaporative cooling. While evaporative cooling exhibits a higher peak power from a static perspective, its sustainability from a dynamic point is limited. Initially, radiative cooling dominates because the module temperature is insufficient to trigger rapid water desorption. As the temperature rises, however, the high enthalpy of vaporization causes evaporative cooling to surpass radiative cooling for a significant period. Eventually, as the water content within the hydrogel diminishes, radiative cooling begins to prevail again.

Fig. 4(c) examines the combined energy contribution of radiative and evaporative cooling against the performance of individual cooling configurations over time. Obviously, the combined cooling energy from both mechanisms is generally lower than the sum of their individual contributions when operated separately. This discrepancy becomes more pronounced as evaporative cooling begins to dominate, leading to an increasing negative value. In the later stages of the cooling process, because of water-saving effect, the hybrid system continues to provide evaporative cooling after the standalone evaporative system has dehydrated and ceased to function, causing the difference to turn positive. This phenomenon can be attributed to a synergistic interaction: the presence of radiative cooling moderates the rate of evaporative energy release, thereby slowing the depletion of water content and extending the effective cooling duration. Such an interaction not only enhances its overall energy efficiency under dynamic conditions but also prolongs the operational lifespan of the cooling system with a shorter duration of complete dehydration, which has great impact on mechanical performance of hydrogel. Thus, radiative cooling could be a valuable supplement to PV modules, working in concert with evaporative cooling as the primary mechanism to ensure sustained passive cooling.

4. CONCLUSIONS

This study provides an in-depth investigation into the synergistic strategy of combined radiative and evaporative cooling for PV thermal management using a validated numerical model. The two mechanisms play complementary roles: evaporative cooling delivers immediate and potent heat removal, while radiative cooling ensures sustained temperature regulation. The hybrid configuration achieved the average temperature reduction of 3.2°C, yielding a 500% greater efficiency increase compared to radiative cooling alone and a

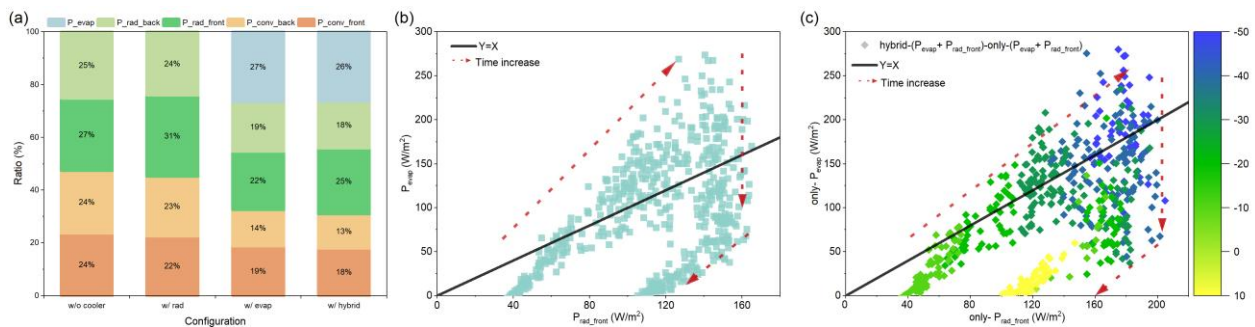


Fig. 4 (a): Energy distribution at 12 p.m.; (b): Energy point at different moment in a single day; (c): Comparison of hybrid and single configurations.

further 26% improvement over evaporative cooling. Furthermore, the hybrid system extended the cooling duration by 10%, as the radiative cooling component moderated the evaporation rate, thereby conserving water content and prolonging the operational period. These findings quantify the cooling potential of the synergy, establishing the feasibility of using radiative cooling as a supplement that sustains evaporative cooling as the primary passive mechanism.

ACKNOWLEDGEMENT

This work is supported by the financial support from the Science and Technology Commission of Shanghai Municipality through Grant 22160713800, and the China National Offshore Oil Corporation Gas and Power Group through Grant CGP2024YFCB025.

REFERENCE

- [1] IEA. Global Energy Review 2025. Paris: 2025.
- [2] Khan SY, Rauf S, Liu S, Chen W, Shen Y, Kumar M. Revolutionizing the solar photovoltaic efficiency: a comprehensive review on the cutting-edge thermal management methods for advanced and conventional solar photovoltaics. *Energy Environ Sci* 2025; 18:1130–75. <https://doi.org/10.1039/D4EE03525A>.
- [3] Dida M, Boughali S, Bechki D, Bouguettaia H. Experimental investigation of a passive cooling system for photovoltaic modules efficiency improvement in hot and arid regions. *Energy Conversion and Management* 2021;243:114328. <https://doi.org/10.1016/j.enconman.2021.114328>.
- [4] Liu J, Zhou Y, Zhou Z, Du Y, Wang C, Yang X, et al. Passive Photovoltaic Cooling: Advances Toward Low-Temperature Operation. *Advanced Energy Materials* 2024;14:2302662. <https://doi.org/10.1002/aenm.202302662>.
- [5] Zhao D, Aili A, Zhai Y, Xu S, Tan G, Yin X, et al. Radiative sky cooling: Fundamental principles, materials, and applications. *Applied Physics Reviews* 2019;6:021306. <https://doi.org/10.1063/1.5087281>.
- [6] Li Z, Ahmed S, Ma T. Investigating the Effect of Radiative Cooling on the Operating Temperature of Photovoltaic Modules. *Solar RRL* 2021;5:2000735. <https://doi.org/10.1002/solr.202000735>.
- [7] Li T, Ma T, Yu K, Peng J. Radiation regulation of silicon photovoltaic modules for effective thermal management: A potential analysis. *Applied Energy* 2025;399:126470. <https://doi.org/10.1016/j.apenergy.2025.126470>.
- [8] Li Z, Ma T, Ji F, Shan H, Dai Y, Wang R. A Hygroscopic Composite Backplate Enabling Passive Cooling of Photovoltaic Panels. *ACS Energy Lett* 2023;8:1921–8. <https://doi.org/10.1021/acscenergylett.3c00196>.
- [9] Mao Z, Yao Y, He Y, Yu Z, Han Y, Shen J, et al. Passively Ultra Cooling Patch Enabling High-Efficiency Power-Water Cogeneration. *Advanced Materials* 2025:e05002. <https://doi.org/10.1002/adma.202505002>.
- [10] Yang X, Chen Y, Zhou Z, Du Y, Wang C, Liu J, et al. Enhancing photovoltaic power generation through hydrogel-based passive cooling: Theoretical model and global application potential. *Appl Energy* 2024;376:124174. <https://doi.org/10.1016/j.apenergy.2024.124174>.
- [11] Huang K, Lan H, Li S, Tan R, Si Y, Lei L, et al. Advanced evaporative cooling materials: From designs to applications. *Progress in Materials Science* 2025;154:101504. <https://doi.org/10.1016/j.pmatsci.2025.101504>.
- [12] Yu X, Liang M, Dong C, Zhang L-Z. Hygroscopic hydrogel-based cooling system for photovoltaic panels: An experimental and numerical study. *Appl Therm Engineering* 2024:124400. <https://doi.org/10.1016/j.applthermaleng.2024.124400>.
- [13] Li H, Ma J, Yan W, Lan J, Hong W. Lithium-based water-absorbent hydrogel with a high solar cell cooling flux. *Renew Energy* 2024:121277. <https://doi.org/10.1016/j.renene.2024.121277>.
- [14] Shang J, Zhang J, Zhang Y, Zhang X, An Q. Highly Potent Transparent Passive Cooling Coating via Microphase-Separated Hydrogel Combining Radiative and Evaporative Cooling. *Nano Lett* 2024. <https://doi.org/10.1021/acs.nanolett.4c01621>.
- [15] Li S, Wang S, Zhao J, Wang Z, Murto P, Yu L, et al. Spectrally-Tailored Hygroscopic Hydrogels with Janus Interfaces for Hybrid Passive Cooling of Solar Cells. *Small* 2025. <https://doi.org/10.1002/smll.202505647>.
- [16] Gu W, Ma T, Shen L, Li M, Zhang Y, Zhang W. Coupled electrical-thermal modelling of photovoltaic modules under dynamic conditions. *Energy* 2019;188:116043. <https://doi.org/10.1016/j.energy.2019.116043>.
- [17] Díaz-Marín CD, Zhang L, Lu Z, Alshrah M, Grossman JC, Wang EN. Kinetics of Sorption in Hygroscopic Hydrogels. *Nano Lett* 2022;22:1100–7. <https://doi.org/10.1021/acs.nanolett.1c04216>.